High-order Arbitrary-Lagrangian-Eulerian schemes on *crazy* moving Voronoi meshes

Elena Gaburro and Simone Chiocchetti

Abstract Hyperbolic partial differential equations (PDEs) cover a wide range of interesting phenomena, from *human* and *hearth*-sciences up to *astrophysics*: this unavoidably requires the treatment of many space and time scales in order to describe at the same time *observer-size* macrostructures, *multi-scale* turbulent features, and also *zero-scale* shocks. Moreover, numerical methods for solving hyperbolic PDEs must reliably handle different families of waves: smooth *rarefactions*, and discontinuities of *shock* and *contact* type. In order to achieve these goals, an effective approach consists in the combination of space-time-based *high-order* schemes, very accurate on smooth features even on coarse grids, with *Lagrangian* methods, which, by moving the mesh with the fluid flow, yield highly resolved and minimally dissipative results on both shocks and contacts. However, ensuring the high quality of *moving meshes* is a huge challenge that needs the development of innovative and unconventional techniques. The scheme proposed here falls into the family of Arbitrary-Lagrangian-Eulerian (ALE) methods, with the unique additional freedom of evolving the *shape* of the mesh elements through connectivity changes. We aim here at showing, by simple and very salient examples, the capabilities of high-order ALE schemes, and of our novel technique, based on the high-order space-time treatment of *topology changes*.

Elena Gaburro

Inria, Univ. Bordeaux, CNRS, Bordeaux INP, IMB, UMR 5251, 200 Avenue de la Vieille Tour, 33405 Talence cedex, France, e-mail: elena.gaburro@inria.fr

Simone Chiocchetti

Department of Civil, Environmental and Mechanical Engineering, University of Trento, Via Mesiano, 77 - I-38123 Trento, Italy. e-mail: simone.chiocchetti@unitn.it

1 Introduction

In order to reduce as much as possible the numerical errors due to nonlinear convective terms, it is possible to exploit the power of Lagrangian methods: with this kind of algorithms, the new position and configuration of each element of the mesh is re-computed at each timestep according to the local fluid velocity, so that we can closely follow the fluid flow in a Lagrangian fashion. In this way the nonlinear convective terms disappear and Lagrangian schemes exhibit *negligible numerical dissipation* at *contact* waves and material *interfaces*; moreover they results to be *Galilean and rotational invariant*, and they provide, without any additional effort, an automatic *mesh refinement* feature even when the cell count is maintained constant, simply by transporting the mesh elements wherever needed.

The use of Lagrangian methods dates back to the works of [65, 67] and then many further improvements have been introduced in literature; we cite here only some few relevant historical examples and review papers [51, 10, 46, 11, 48, 42, 59, 17, 16, 49].

However, ensuring the high quality of a *moving mesh* over long simulation times is difficult, therefore a certain degree of flexibility should be allowed in order to avoid mesh distortion, for example a slightly relaxed choice of the actual mesh velocity w.r.t the real fluid velocity, as well as the freedom of not only *moving* the control volumes, but really *evolving* their shapes and allowing topology and neighborhood changes. This led to the introduction of Arbitrary-Lagrangian-Eulerian (ALE) schemes of *direct* [19, 6, 8] and *indirect* [45, 44, 5] type. In particular, as stated and shown in [61], connectivity changes between different time level constitute a valid alternative to remeshing [44, 5, 45] for preserving or restoring mesh quality in a Lagrangian setting.

With this in mind, we present here a novel family of very *high-order* direct Arbitrary-Lagrangian-Eulerian (ALE) Discontinuous Galerkin (DG) schemes for the solution of general nonlinear hyperbolic PDE systems on moving Voronoi meshes that are *regenerated* at each timestep and which explicitly allow *topology changes* in time, in order to benefit simultaneously from high-order methods, high quality grids and substantially reduced numerical dissipation; this method has been introduced for the first time by the two authors in [28].

The *key ingredient* of our approach is the integration of a *space-time conservation formulation* of the governing PDE system over closed, non-overlapping *space-time* control volumes [8] that are constructed from the moving, *regenerated*, Voronoi-type polygonal meshes which are centroid-based dual grids of the Delaunay triangulation of a set of *generator* points: this leads to also consider what we refer to in this work as *crazy degenerate* control volumes, or *space-time sliver* elements, that only arise when adopting a space-time framework, and would not exist from a purely spatial point of view! Such degenerate elements provide a clear formal way of handling mesh connectivity changes while preserving the high-order of accuracy of the numerical method.

1.1 Goals

The goal of this book chapter is to briefly review this novel and promising approach based on high order direct ALE schemes with topology changes, and to provide numerical evidence regarding the utility of Lagrangian methods in general, and in particular of the new technique object of this work, by means of simple and illustrative benchmarks.

1.2 Structure

The rest of this chapter is organized as follows. We first introduce the class of equations of interest in Section 2. Next, we briefly summarize the main characteristics of the employed direct Arbitrary-Lagrangian-Eulerian scheme, focusing in particular on the space-time approach and its extension to *crazy* sliver elements, whose formation, caused by topology changes, will be also addressed in Section 3.2. Then, the core of this work consists in providing numerical evidence for *(i)* the key role of topology changes and sliver elements in a high-order moving mesh code, and *(ii)* the clear advantages of Lagrangian schemes on widely adopted benchmark problems. Finally, we give some conclusive remarks and an outlook towards future work in Section 5.

2 Hyperbolic partial differential equations

In order to model a wide class of physical phenomena, we consider a very general formulation of the governing equations, namely all those which can be described by

$$\partial_t \mathbf{Q} + \nabla \cdot \mathbf{F}(\mathbf{Q}) + \mathbf{B}(\mathbf{Q}) \cdot \nabla \mathbf{Q} = \mathbf{S}(\mathbf{Q}), \tag{1}$$

where $\mathbf{Q}$ is the vector of the conserved variables, $\mathbf{F}$ the non linear flux, $\mathbf{B} \cdot \nabla \mathbf{Q}$ the non-conservative products, and $\mathbf{S}$ a nonlinear algebraic source term. Many physical models can be cast in this form, from the simple shallow water system, some multiphase flow models, the magnetohydrodynamics equations, up to the Einstein field equations of general relativity (with appropriate reformulation) or the GPR unified model of continuum mechanics, see for example [25, 29, 38, 30, 14, 62, 13, 14, 26, 54, 7]; in this work, we will present illustrative results concerning the Euler equations of gasdynamics.

3 Numerical method

In this Section we presents a concise description of our direct Arbitrary-Lagrangian-Eulerian (ALE) Discontinuous Galerkin (DG) scheme on moving Voronoi-type meshes with topology changes; for any additional details we refer to our recent paper [28].

At the beginning of the simulation, we discretize our moving domain by a centroid-based Voronoi-type tessellation built from a set of generators (the orange points in Figure 1), and we represent our data, the conserved variables $\mathbf{Q}$, via discontinuous high-order polynomials in each mesh polygon (we indicate the degree of the polynomial representation by P_N). Then, we let the generators move with a velocity chosen to be as close as possible to the local fluid velocity, computed mainly from a high-order approximation of their pure Lagrangian trajectories, with small corrections obtained from a flow-adaptive mesh optimization technique. The positions of the generators are being continuously updated, and thus their Delaunay triangulation may change at any timestep and the same will hold for the dual polygonal tessellation. Then, a space-time connection between two polygonal tessellations corresponding to two successive time levels has to be established in order to evolve the solution in time locally and integrate the governing PDE.

3.1 Direct Arbitrary-Lagrangian-Eulerian schemes

The key idea of *direct* ALE methods (in contrast to *indirect* ones) consists in connecting two tessellations by means of so-called *space-time control volumes* C_i^n, and recover the unknown solution at the new timestep $\mathbf{u}_h^{n+1}$ *directly* inside the new polygon P_i^{n+1}, from the data available at the previous timestep $\mathbf{u}_h^n$ in P_i^n. This is achieved through the *integration*, over such control volumes, of the fluxes, the non-conservative products and the source terms, by means of a high-order fully discrete predictor-corrector ADER method [21, 31]. In this way, the need for any further
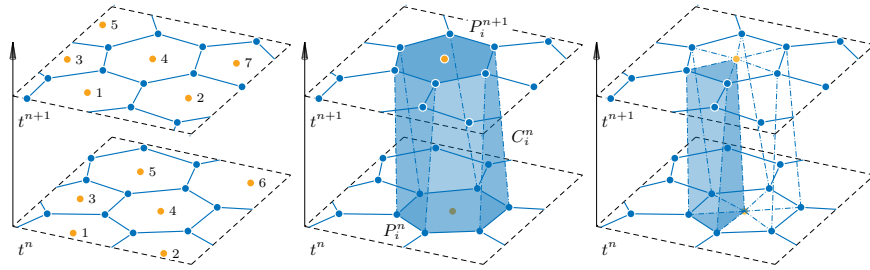

Fig. 1 Space time connectivity *without* topology changes, main space-time control volume (middle) and a standard sub-space-time control volume (right).

remapping/remeshing steps is totally eliminated. By adopting the tilde symbol for referring to space-time quantities, our direct ALE scheme [28, 27] reads

$$\int_{P_i^{n+1}} \tilde{\phi}_k \mathbf{u}_h^{n+1} = \int_{P_i^n} \tilde{\phi}_k \mathbf{u}_h^n - \sum_j \int_{\partial C_{ij}^n} \tilde{\phi}_k \mathcal{F}(\mathbf{q}_h^{n,-}, \mathbf{q}_h^{n,+}) \cdot \tilde{\mathbf{n}} + \int_{C_i^n} \tilde{\nabla} \tilde{\phi}_k \cdot \tilde{\mathbf{F}}(\mathbf{q}_h^n)$$
$$+ \int_{C_i^n} \tilde{\phi}_k \left(\mathbf{S}(\mathbf{q}_h^n) - \tilde{\mathbf{B}}(\mathbf{q}_h^n) \cdot \nabla \mathbf{q}_h^n \right), \tag{2}$$

where $\tilde{\phi}_k$ is a set of moving space-time basis functions, while $\mathbf{q}_h^{n,+}$ and $\mathbf{q}_h^{n,-}$ are high-order space-time extrapolated data computed through the ADER predictor. Finally, $\mathcal{F}(\mathbf{q}_h^{n,-}, \mathbf{q}_h^{n,+})$ is an ALE numerical flux function which takes into account fluxes across space-time cell boundaries ∂C_{ij}^n as well as jump terms related to nonconservative products. In particular, we adopt here a two-point path-conservative numerical flux function of Rusanov-type [58, 53]

$$\mathcal{F}(\mathbf{q}_h^{n,-}, \mathbf{q}_h^{n,+}) \cdot \tilde{\mathbf{n}} = \frac{1}{2} \left(\tilde{\mathbf{F}}(\mathbf{q}_h^{n,+}) + \tilde{\mathbf{F}}(\mathbf{q}_h^{n,-}) \right) \cdot \tilde{\mathbf{n}}_{ij} - \frac{1}{2} s_{\max} \left(\mathbf{q}_h^{n,+} - \mathbf{q}_h^{n,-} \right)$$
$$+ \frac{1}{2} \left(\int_0^1 \tilde{\mathbf{B}} \left(\mathbf{\Psi}(\mathbf{q}_h^{n,-}, \mathbf{q}_h^{n,+}, s) \right) \cdot \mathbf{n} \, d\mathbf{x} \right) \cdot \left(\mathbf{q}_h^{n,+} - \mathbf{q}_h^{n,-} \right), \tag{3}$$

where $s_{\max}$ is the maximum eigenvalue of the *ALE Jacobian matrices* evaluated on the left and right of the space-time interface and the path $\mathbf{\Psi} = \mathbf{\Psi}(\mathbf{q}_h^-, \mathbf{q}_h^+, s)$ is a straight-line segment path connecting $\mathbf{q}_h^{n,-}$ and $\mathbf{q}_h^{n,+}$.

We emphasize that the ALE Jacobian matrix is obtained by subtracting the local normal mesh velocity from the diagonal entries of the system matrix of the quasi-linear form of the governing equations [63] (the Jacobian of the interface-normal flux for conservative systems), thus, when the mesh velocity is sufficiently close to the local fluid velocity, the wavespeed estimates obtained from the eigenvalues are significantly reduced, leading to a lower associated numerical dissipation than what would be mandated in the Eulerian context. This, especially but not exclusively, in conjunction with complete approximate Riemann solvers [20], explains the capability of tracking material interfaces and capturing contact discontinuities which are characteristic of Lagrangian-type schemes.

Next, in order to compute the integrals with high order of accuracy, complete knowledge of the *space-time connectivity* between two consecutive timesteps is required, as opposed to only the *spatial* information at the two time levels, which would be enough for a low order scheme [61] or for indirect schemes [45, 44, 5].

When no topology changes occur, the space-time geometrical information is easily constructed by connecting via straight line segments the corresponding vertexes of each polygon, obtaining an oblique prism than can be further subdivided into a set of triangular oblique sub-prisms on which quadrature points are readily available (see Figures 1 and 3).

3.2 Topology changes and *crazy* sliver elements

On the contrary, when a topology change occurs, as in Figure 2, i.e. the number of edges, the shape, and the neighbors of a polygon evolve within two consecutive timesteps, the space-time connection between the mesh elements gives raise to degenerate elements of two types: *(i) degenerate sub*-space-time control volumes, where either the top or bottom faces are degenerate triangles that are collapsed to a segment; *(ii)* and also *crazy sliver* space-time elements S_i^n. The first type of degenerate elements does not pose any problems, and was already treated in [32]. Instead, space-time sliver elements are a completely new type of control volume. In particular, they do not exist neither at time t^n, nor at time t^{n+1}, since they coincide with an edge of the tessellation at the old *and* at the new time levels, and for this reason have zero area in space at the two bounding time levels. However, they have a *non-negligible volume* in space-time. The difficulties related to this kind of elements are due to the fact that for them an initial condition is not clearly defined at time t^n, and that contributions across these elements should not be lost at time t^{n+1}, in order to ensure conservation. All the details on how to successfully extend our direct ALE scheme also to *crazy* elements can be found in our recent paper [28].
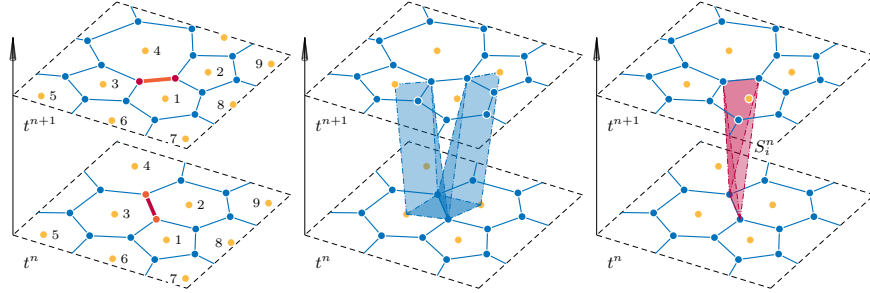

Fig. 2 Space time connectivity *with* topology changes, degenerate sub-space-time control volumes (middle) and *crazy* sliver element (right).
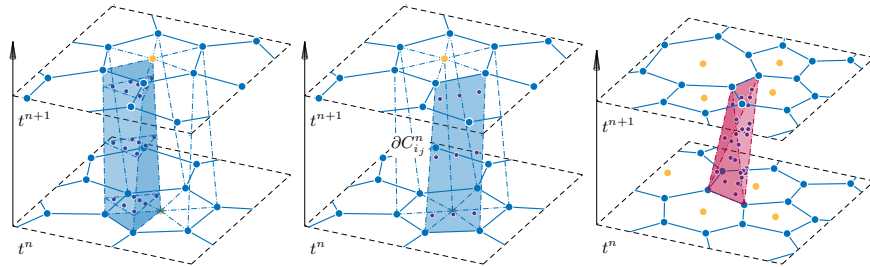

Fig. 3 Space-time quadrature points for third order methods on standard elements (left), lateral faces (middle) and *crazy* sliver elements (right).

We would like to emphasize that topology changes are fundamental for long time simulations in the ALE framework, in order to avoid explicit data remap steps, and our *crazy* sliver elements represent a *novel and formally grounded* way to allow for a relatively simple space-time connection around a change of connectivity. The numerical results shown in Section 4.1 provide a clear proof of the necessity of topology changes already on the simple situation of the long time evolution of a stationary isentropic smooth vortex.

3.3 ADER-ALE algorithm: the predictor step

The *predictor* step represents an essential ingredient for obtaining high-order in time in a fully-discrete one-step procedure: it yields a *local* solution of the governing equations (1) *in the small* $\mathbf{q}_h^n$, inside each space-time element, including the *crazy* elements. The solution is *local* in the sense that it is obtained by only considering the initial data in each polygon, the governing equations and the geometry of C_i^n, without taking into account interactions between C_i^n and its neighbors. Such local solution is computed for each standard space-time control volume C_i^n and for each *crazy* control volume S_i^n, in the form of a high order polynomial *in space and in time*, which serves as a predictor solution, to be used for evaluating all the integrals in the *corrector* step (2), i.e. the final update of the solution from t^n to t^{n+1}.

3.4 *A posteriori* sub-cell FV limiter

High-order schemes that can be seen as linear in the sense of Godunov [34], may develop spurious oscillations in presence of discontinuities. In order to prevent this phenomenon, in the case of a DG discretization we adopt an *a posteriori* limiting procedure based on the MOOD paradigm [15, 47, 31]: we first apply our unlimited ALE-DG scheme everywhere, and then (*a posteriori*), at the end of each timestep, we check the reliability of the obtained solution in each cell against physical and numerical admissibility criteria, such as floating point exceptions, violation of positivity or violation of a relaxed discrete maximum principle (and see [35, 39] for further criteria). Next, we mark as *troubled* those cells where the DG solution cannot be accepted. For the troubled cells we now repeat the time evolution by employing, instead of the DG scheme, a more robust finite volume (FV) method. Moreover, in order to maintain the accurate resolution of our original high-order DG scheme, which would be lost when switching to a FV scheme, the FV scheme is applied on a *finer sub-cell grid* that accounts for recovering the optimal accuracy of the numerical method performing a reconstruction step.

4 Numerical examples

In order to provide simple and clear numerical evidence of the effectiveness of the proposed ALE scheme with topology changes we consider here the well known Euler equations, that can be cast in the form (1) by choosing

$$
\mathbf{Q} = \begin{pmatrix} \rho \\ \rho u \\ \rho v \\ \rho E \end{pmatrix}, \quad \mathbf{F} = \begin{pmatrix} \rho u & \rho v \\ \rho u^2 + p & \rho uv \\ \rho uv & \rho v^2 + p \\ u(\rho E + p) & v(\rho E + p) \end{pmatrix}, \quad \mathbf{B} = \mathbf{0}, \quad \mathbf{S} = \mathbf{0}. \quad (4)
$$

The vector of conserved variables $\mathbf{Q}$ is composed of the fluid density ρ, the momentum density vector $\rho \mathbf{v} = (\rho u, \rho v)$ and the total energy density ρE; next, the fluid pressure p is computed using the equation of state for an ideal gas

$$
p = (\gamma - 1) \left(\rho E - \frac{1}{2} \rho \mathbf{v}^2 \right), \quad (5)
$$

where γ (in this work taken to be $\gamma = 7/5$) is the ratio of specific heats. For this choice of equation of state, the adiabatic speed of sound takes the form $c = \sqrt{\gamma p / \rho}$.

In what follows we will present numerical results regarding the following notable features of Lagrangian schemes and of our direct Arbitrary-Lagrangian-Eulerian method with variable topology:

i.   Flows characterized by strong differential rotations, for example vortices, can be studied over very long periods only by conceding to the element motion the additional freedom of introducing topology changes, see Section 4.1;

ii. The use of sliver elements allows to clearly define the space-time evolution of the solutions in-between discrete time levels and achieves high-order of accuracy also in presence of many topology changes, see Section 4.1.1;

iii. Lagrangian schemes sharply capture *shock* waves thanks to the automatic refinement obtained at the shock locations without needing to increment the number of mesh elements but simply because the element density increases wherever needed, see Section 4.2;

iv. Lagrangian schemes minimize dissipation of *contact* discontinuities, by applying reduced numerical dissipation when using approximate Riemann solvers. In a pure Lagrangian context, schemes capable of capturing stationary discontinuities exactly will do the same also for moving interfaces (since the mesh motion is specified to follow such features). Moreover, even when such hard constraints are relaxed in Arbitrary-Lagrangian-Eulerian methods and even using simpler solvers like the Rusanov flux, the bounding wavespeed estimates and the associated numerical dissipation can be much lower than what would be mandated in the Eulerian context, see Section 4.3;

v.   Lagrangian schemes discretely preserve the Galilean and rotational invariance properties of the governing equations, so that they can better capture any events

(such as the explosion-type problems reported in this work) that may occur in superposition to a high-speed background flow, see Section 4.3.

4.1 Long time evolution of a Shu-type vortical equilibrium

As a first test we consider a smooth isentropic vortex flow defined as similarly to [36]. The initial computational domain is the square $\Omega = [0; 10] \times [0; 10]$ and boundary conditions are of wall (slip) type everywhere. The initial condition is given by some perturbations δ that are superimposed onto a homogeneous background state $\mathbf{Q}_0 = (\rho, u, v, p) = (1, 0, 0, 1)$, assuming that the entropy perturbation is zero, i.e. $\delta S = 0$. The perturbations for density and pressure are

$$\delta \rho = (1 + \delta T)^{\frac{1}{\gamma-1}} - 1, \quad \delta p = (1 + \delta T)^{\frac{\gamma}{\gamma-1}} - 1, \tag{6}$$

with the temperature fluctuation $\delta T = -\frac{(\gamma-1)\,\epsilon^2}{8\gamma\pi^2}e^{1-r^2}$ and the vortex strength $\epsilon = 5$. The velocity field is specified by
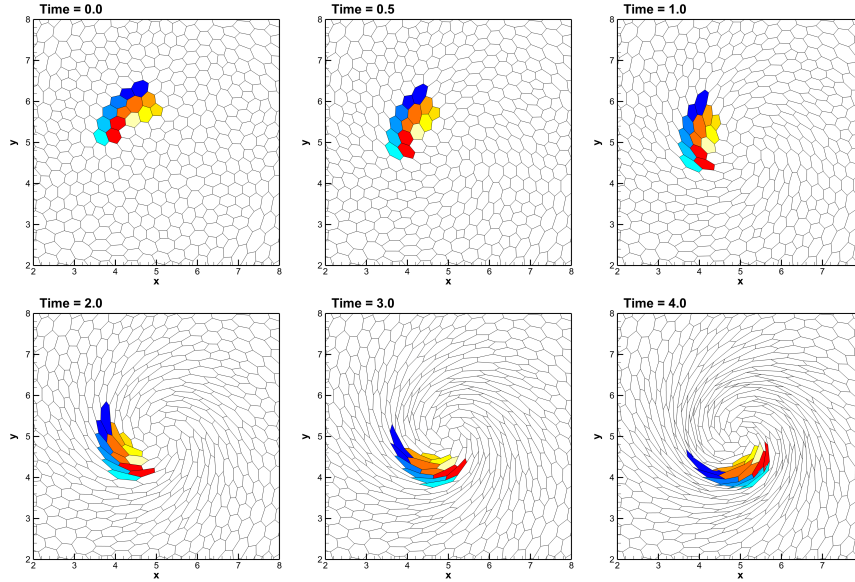

Fig. 4 Mesh evolution corresponding to the solution of the stationary rotating vortex of Section 4.1 solved on a moving grid with *fixed* topology. The mesh quality rapidly deteriorates: elements are stretched, the timestep size is reduced, and even mesh-tangling occurs, which means that the simulation may stop entirely.

$$\begin{pmatrix} \delta u \\ \delta v \end{pmatrix} = \frac{\epsilon}{2\pi} e^{\frac{1-r^2}{2}} \begin{pmatrix} -(y-5) \\ (x-5) \end{pmatrix}. \tag{7}$$

This is a stationary equilibrium of the system so the exact solution coincides with the initial condition at any time.

Preserving this kind of vortical solution over long simulation times with minimal dissipation is a nontrivial task in a moving-mesh context. To achieve this result, we propose the use of a very high-order scheme (here an ADER-DG method of order 4) in a Lagrangian framework. We remark that the combination cannot be used with fixed topology, or advanced remapping techniques, because the quality of the moving mesh subject to this constraint quickly deteriorates, as is clearly apparent in Figure 4, where the simulation has to be stopped after about half a vortex rotation
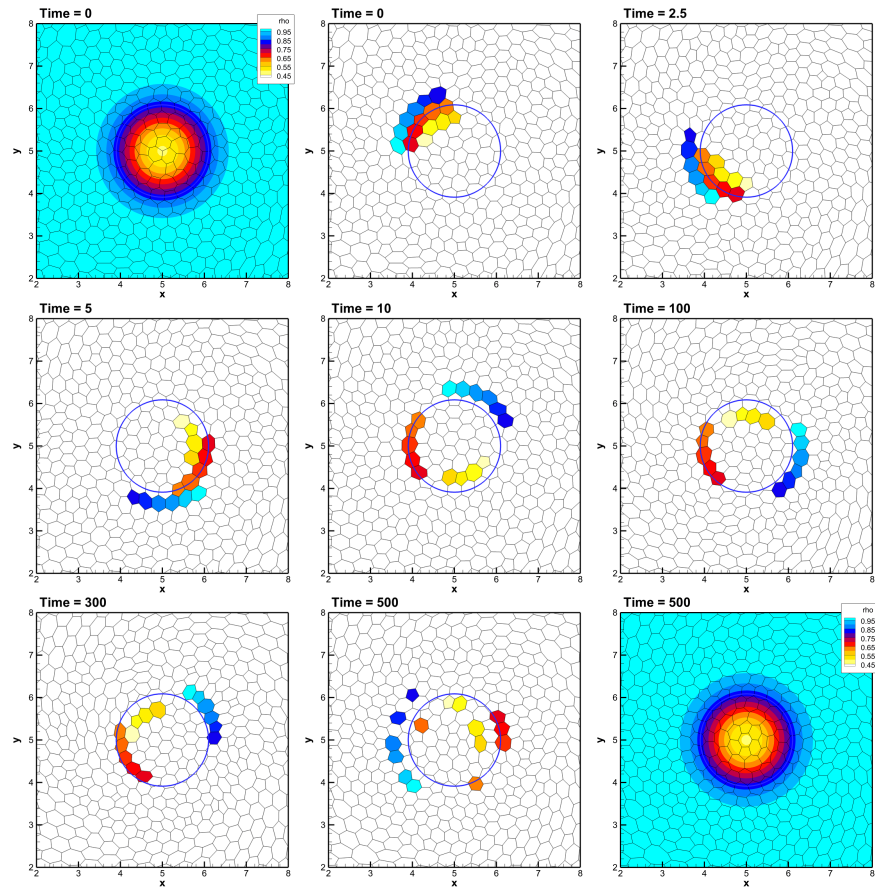

Fig. 5 Stationary rotating vortex solved with our fourth order ALE-DG scheme. Density contours at $t = 0$ and $t = 500$ and position of a bunch of highlighted elements at different times. Note that the solution is well preserved for more than *eighty* complete rotation periods of the yellow elements and generator trajectories are perfectly circular.

period. This highlights the well-known fact that, for long time evolution, the mesh connectivity must be somehow updated. In this work this is naturally achieved by means of space-time topology changes.

Further, Figure 5 demonstrates that the treatment of topology changes via high-order integration over *crazy* sliver elements is actually quite effective. Indeed one can note that the solution is visually the same at the beginning of the simulation and 500 seconds after, even on a rather coarse mesh of only 957 polygonal elements. More-over, we take advantage of this test case to also emphasize the high precision of the mesh movement. The Voronoi-type polygonal cells, as well as the generator points, in fact can be observed to orbit along perfectly circular trajectories, as evidenced in Figures 5 and 6.

4.1.1 Order of convergence

Finally, this stationary test case allows to show numerically the order of convergence of the proposed ALE-DG scheme with topology changes, reported in Table 1 up to order 4. Furthermore, we present a quantitative comparison with the scheme applied in a purely Eulerian setting (i.e. on a fixed mesh) and with the classical direct ALE approach with fixed topology. For the purpose of this test, we consider the domain $\Omega = [-10; 30] \times [-10; 30]$, covered with a Voronoi-type tessellation obtained as
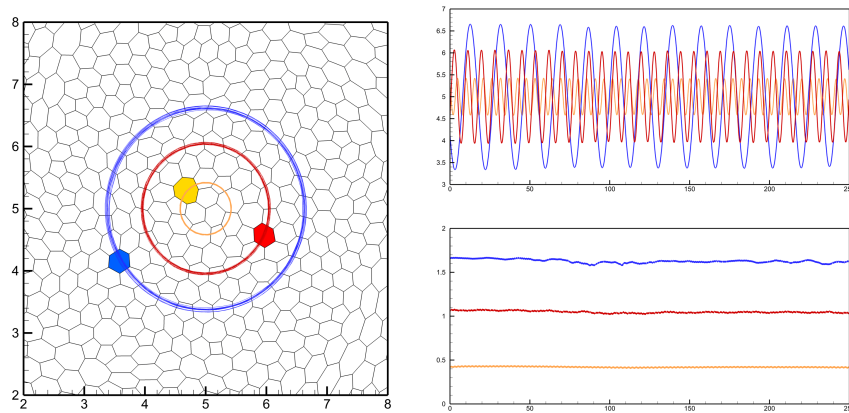

Fig. 6 Stationary rotating vortex solved with our fourth order P_3 ALE-DG scheme on a moving Voronoi-type mesh of 957 elements with dynamical change of connectivity and with the generators trajectories computed with fourth order of accuracy. Left: We depict the trajectories (in Cartesian coordinates) of the generators of 3 mesh elements (those highlighted respectively in blue, violet and red) from time $t = 0$ up to time $t = 250$. During this time interval the red mesh element completes 30 revolutions about the origin. Right: we depict the y coordinates of the 3 generators (top) and their radial coordinates (bottom). We would like to emphasize that the trajectories are circular (their radius is almost constant) for a very long evolution time.

Table 1 Stationary vortex test case with final time $t = 4$ and $t = 10$. We report here the order of convergence, on the variable ρ in the L_2 norm, for our DG scheme up to order 4 in the Eulerian case (left), for a standard Lagrangian method with fixed topology (middle) and for our ALE scheme with topology changes (right). In the last case we also report the total number of *crazy* sliver elements that have been originated during the simulations: the high order of convergence is maintained also when many sliver elements appear in the mesh. At large times ($t = 10$), the ALE scheme with topology changes, produces numerical errors that are comparable or smaller than those obtained with the corresponding Eulerian method on a fixed mesh.

| | | Eulerian | | | ALE fixed | | ALE+sliver | | | | |
| | | t=4 | t=10 | | t=4 | | t=4 | | t=10 | | |
	h	$\epsilon(\rho)$	$\epsilon(\rho)$	$O(L_2)$	$\epsilon(\rho)$	$O(L_2)$	Sliv	$\epsilon(\rho)$	Sliv	$\epsilon(\rho)$	$O(L_2)$
$P_1 \to O2$	5.9E-1	4.7E-2	8.3E-2	-	1.4E-1	-	111	4.8E-2	293	9.0E-2	-
	4.4E-1	2.8E-2	4.6E-2	2.0	1.1E-1	1.0	192	2.4E-2	514	4.3E-2	2.6
	2.9E-1	1.0E-2	1.8E-2	2.4	4.6E-2	2.1	420	9.3E-3	1119	1.5E-2	2.6
	2.2E-1	4.9E-3	8.0E-3	2.8	2.4E-2	2.3	789	4.6E-3	2111	6.5E-3	2.9
$P_2 \to O3$	5.9E-1	6.7E-3	1.1E-2	-	2.7E-2	-	97	7.3E-3	277	1.0E-2	-
	4.4E-1	2.8E-3	3.9E-3	3.6	1.3E-2	2.5	181	2.9E-3	498	3.2E-3	4.0
	2.9E-1	9.6E-4	1.1E-3	3.3	6.8E-3	1.6	401	9.7E-4	1066	9.0E-4	3.2
	2.2E-1	4.0E-4	4.1E-4	3.4	3.3E-3	2.5	745	4.3E-4	1981	4.1E-4	2.8
$P_3 \to O4$	1.7E-0	5.6E-2	8.0E-2	-	5.8E-2	-	2	5.3E-2	4	6.8E-2	-
	1.1E-0	1.2E-2	2.2E-2	3.2	2.8E-2	1.8	10	1.3E-2	41	1.9E-2	3.2
	8.7E-1	4.7E-3	6.6E-3	4.4	2.0E-2	1.3	36	5.8E-3	110	6.1E-3	4.2
	5.9E-1	1.1E-3	1.3E-3	4.2	5.4E-3	3.3	93	1.1E-3	257	1.3E-3	3.9

the centroid-based dual of a Delaunay mesh generated by Ruppert's algorithm [57]. We report our results at time $t = 4$ (the time at which the ALE simulations with fixed topology terminate due to mesh tangling) and $t = 10$ (a long simulation time at which differences in mesh configuration become very significant).

It should be stressed that, due to the absence of discontinuous features or strong background flows, this test problem is not intended to highlight the capabilities of moving mesh algorithms, but rather to show the high order convergence of the method on smooth flows, while highlighting the necessity for a changing mesh topology.

On the results, we note that the ALE method applied to a fixed mesh topology, in addition to early termination around time $t = 4$, as shown in Figure 4, also suffers an increase in numerical errors, to the point that the correct order of convergence cannot be obtained when the mesh is severely tangled. Instead, the ALE algorithm presented in this work, not only deals with topology changes without accuracy losses, but in fact the mesh motion allows to gradually optimize the shape of the elements with respect to the flow field. This gradual optimization procedure, translates into lower errors at large times with respect to the Eulerian scheme, for which the mesh is fixed to its initial generic configuration. We refer also to Figure 7 for a visual illustration of the different mesh motion approaches.

Finally, we would like to emphasize that in Table 1 we show the numerical errors obtained at large computational times ($t = 4$ and $t = 10$), when computations have

been carried out for thousands of timesteps and thousands of *crazy* sliver elements have appeared (the total number is indicated in the Table), hence showing that the numerical method is genuinely high order accurate also when sliver elements are present.

4.2 Sedov explosion problem

This test problem is a classic benchmark in the literature [43] and describes the evolution of a strong blast wave that is generated at the origin $\mathbf{O} = (x, y) = (0, 0)$ of the computational domain $\Omega(0) = [0; 1.2] \times [0; 1.2]$. The difficulty of this benchmark is mainly due to the near zero pressure outer state that may induce positivity-preservation problems. An exact solution based on self-similarity arguments is available from [60].

The initial condition consists in a uniform density $\rho_0 = 1$ and a near zero pressure p_0 imposed everywhere except in the cell V_{or} containing the origin $\mathbf{O}$ where it is given by

$$p_{or} = (\gamma - 1)\rho_0 \frac{E_{tot}}{|V_{or}|}, \quad \text{with } E_{tot} = 0.979264, \tag{8}$$

with E_{tot} being the total energy concentrated in the cell containing the coordinate $\mathbf{x} = \mathbf{0}$. We set $p_0 = 10^{-9}$ and solve this numerical test with a fourth order P_3 DG scheme; we employ a coarse mesh $M1$ made of 1345 polygonal cells and a finer mesh $M2$ of 6017 polygonal elements.

The density profiles are shown in Figure 8 for various output times $t = 0.1, 0.5, 1.0$. The obtained results are in perfect agreement with the reference solution and the symmetry is very good despite using an unstructured grid, as opposed to a regular
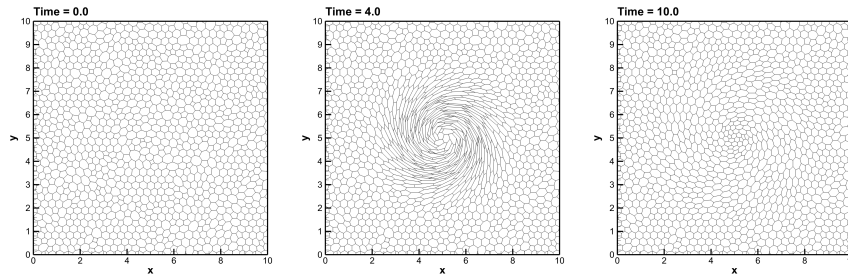

Fig. 7 Stationary vortex test case. We show here an example of a mesh employed for the convergence test case of Section 4.1.1 and of its evolution due to different Lagrangian schemes. In particular, on the left we show the initial mesh, in the middle the mesh obtained with a standard direct ALE scheme with fixed topology at time $t = 4$, i.e. just before the simulation terminates due to mesh tangling, and on the right the mesh obtained at time $t = 10$ with our ALE algorithm dealing with topology changes, which has gradually adapted to the fluid flow, optimizing the element shapes and allowing an increased precision for the DG scheme.
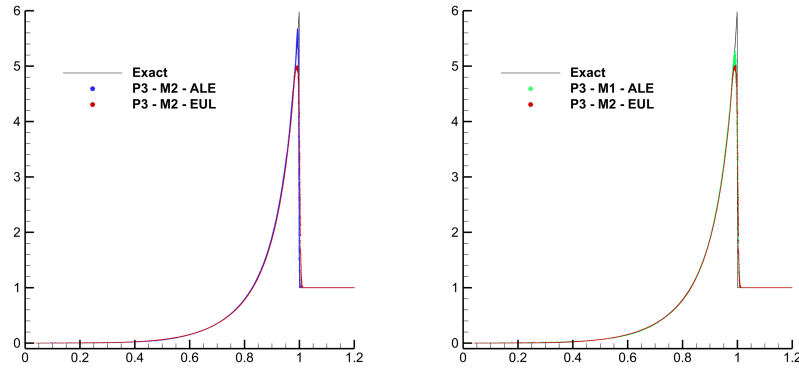
Fig. 8 Sedov explosion problem. Comparison between the exact solution (black), the solution obtained with a fourth order Eulerian P_3 DG method on the fine mesh $M2$ (red) and with our P_3 ALE-DG scheme both on $M2$ (blue) and $M1$ (green). Our ALE scheme is more accurate than the Eulerian one even using coarser meshes.
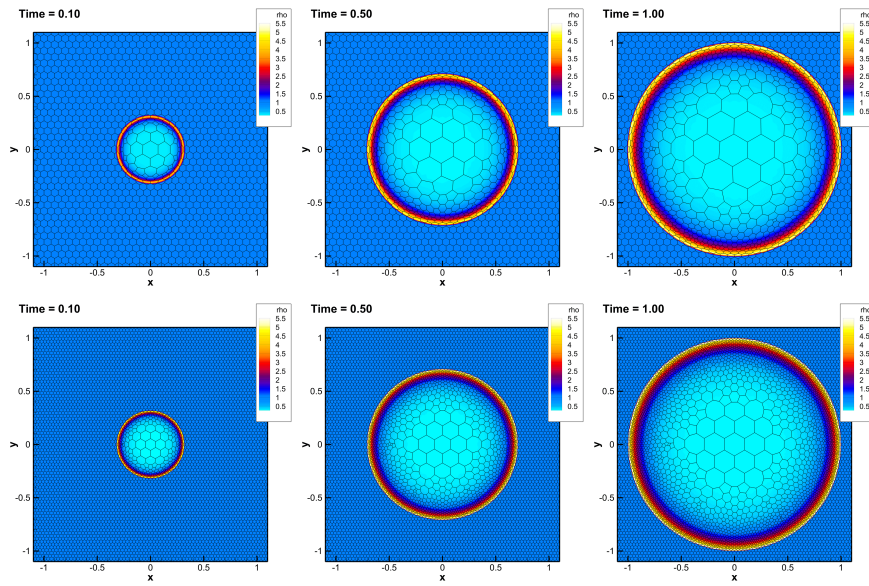

Fig. 9 Sedov explosion problem. In this figure we show the density evolution and the corresponding mesh movement at different output times computed with our P_3 ALE-DG scheme on the mesh $M1$ (top) and $M2$ (bottom).
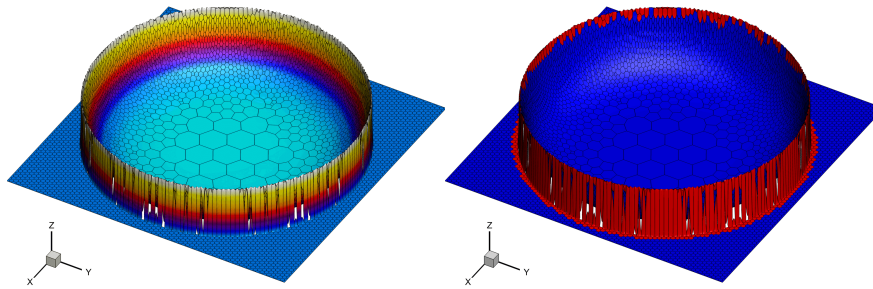
Fig. 10 Sedov explosion problem. $3D$ density profile computed with our P_3 ALE-DG scheme on $M2$. In particular, on the right, we highlight in red the so-called *troubled* cells marked by our detector on which the *a posteriori* FV limiter has been employed. We make use of this image to further emphasize the robustness of our ALE schemes with topology changes also in the presence of strong shock waves and near-zero pressure outer states.

one built in polar coordinates. Also, one can note that the regularization procedure applied to the mesh elements does not compromise the natural expansion of the central cells expected in such an explosion problem. Moreover, one can refer to Figure 10 for a comparison between our numerical solution (scatter plot) and the exact solution: the position of the shock wave and the density peak are perfectly captured.

In particular, we have chosen this test case in order to emphasize that Lagrangian schemes show a superior resolution w.r.t. Eulerian ones even when both are compared at very high-order of accuracy, and furthermore that our direct ALE scheme results more accurate then the Eulerian method, even on a mesh ($M1$) that is coarser by a factor of two with respect to the finer mesh $M2$.

Finally, we refer to Figure 10 for the behavior of our *a posteriori* sub-cell finite volume limiter, which activates only where the shock wave is located and is able to avoid any spurious oscillations or positivity problems, as can be noticed from the precise $3D$ density profile shown in Figure 10.

4.3 Traveling Sod-type explosion problem

The explosion problem can be seen as a multidimensional extension of the classical Sod test case. Here, we consider as computational domain a square of dimension $[-1.1; 1.1] \times [-1.1; 1.1]$ covered with a mesh made of 4105 Voronoi-type elements, and the initial condition is composed of two different states, separated by a discontinuity at radius $r_d = 0.5$

$$\begin{cases} \rho_L = 1, & \mathbf{u}_L, & p_L = 1, & \|\mathbf{x}\| \leq r_d \\ \rho_R = 0.125, & \mathbf{u}_R, & p_R = 0.1, & \|\mathbf{x}\| > r_d. \end{cases} \tag{9}$$

In addition, we aim at capturing the evolution of this explosion over a very high speed moving background (much higher than the speed of sounds): we impose $\mathbf{u}_L = \mathbf{u}_R = 40$, so that at the final simulation time $t_f = 0.25$ the square $[-1; 1] \times [-1; 1]$ will have been displaced by 5 times its initial size.

We would like to underline that this test problem involves three different waves, therefore it allows each ingredient of our Lagrangian scheme to be properly checked. Indeed, we have *(i)* one cylindrical shock wave that is running towards the external boundary: our high-order scheme does not exhibit spurious oscillations thanks to the *a posteriori* sub-cell finite volume limiter; *(i)* a rarefaction fan traveling in the opposite direction, which is well captured thanks to the high-order of accuracy of the DG scheme; and *(iii)* an outward-moving contact wave, which is well resolved thanks to the Lagrangian nature of our scheme, in which, since the mesh moves together with the fluid flow, we can introduce a minimal dissipation when computing approximate Riemann fluxes.
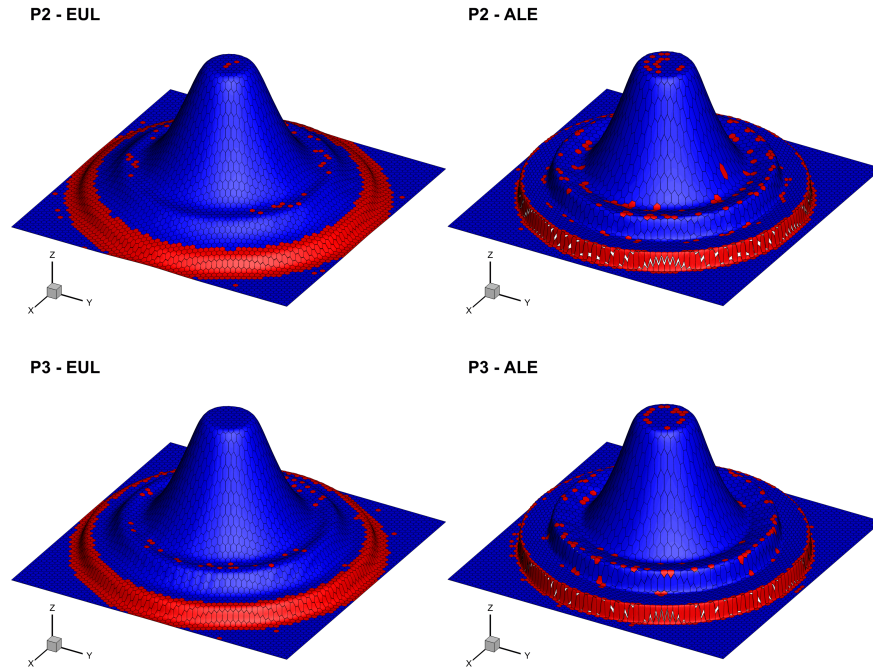

Fig. 11 Traveling Sod explosion problem. $3D$ density profile (z-axis) and limiter activation (red cells), over a domain located in $[8.9; 11.1] \times [-1.1; 1.1]$ at the final time $t_f = 0.25$, obtained with P_2 and P_3 ADER-DG schemes run on a fixed Eulerian mesh (left) and our direct ALE framework with topology changes (right). The difference on the numerical dissipation between the Eulerian and the Lagrangian schemes is quite evident. We clarify that these results are obtained solving the classical Sod explosion problem over a high speed moving background.

In addition, the high speed moving background allows to show the *translational invariance* property of the Lagrangian schemes that indeed perfectly captures the three waves even when the explosion solution is moving at high speed, while the Eulerian scheme is heavily affected by the increased numerical dissipation. Numerical evidence of the above statements can be found in Figure 11; moreover, in Figure 12 we show that for this mild explosion it is really the background motion that requires the use of Lagrangian schemes, which, while still useful, would be instead not fundamental on a fixed background.

Finally, we want to remark that, despite the very high dissipation associated with the high base convective speed, the overall symmetry of the solution, even in the Eulerian case, is not entirely compromised, thanks to the use of polygonal elements (see [9] for further discussion on the benefits of adopting polygonal meshes).

5 Conclusion and outlook

The accuracy of our results clearly show that the new combination of very high-order schemes with regenerated meshes, that allow topology changes, may open new perspectives in the fundamental research field of Lagrangian methods.

We would like to remark that the chosen simple test cases can be seen as prototypes of classical difficulties in astrophysical applications. Indeed, we have proposed here
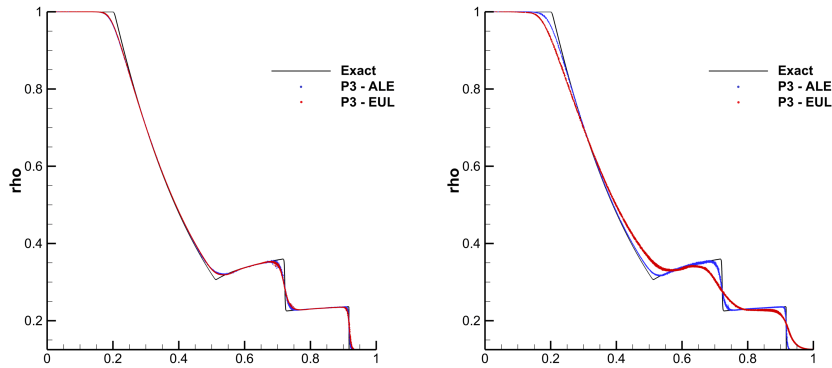

Fig. 12 Sod explosion problem: fixed background (left) and high speed traveling background (right). Comparison between the P_3 DG schemes on fixed Eulerian meshes (red) and in the moving-mesh ALE framework (blue). This numerical results clearly explain that the Lagrangian schemes allow to obtain minimally dissipative results not only in a vanishing background flow, but even in a high speed one, and therefore that Lagrangian methods discretely preserve the Galilean invariance of the equations. On the contrary the influence of strong background flows on the solution obtained with Eulerian schemes is immediately apparent.

a method able to deal with long time simulation of vortical phenomena, as those necessary for the study of gas clouds evolving around black holes and neutron stars, and events, like explosions or interactions with near zero pressure states, occurring in superposition with high speed background flows, as for supersonic or relativistic jets originating from proto-planetary nebulae, binary stars or nuclei of active galaxies.

Future developments of this work will mainly concern the improvements of its robustness and effectiveness through mesh optimization and smoothing techniques [56, 2, 50, 18, 66] and structure preserving algorithms [41, 37, 12, 23, 22, 1, 33] so that future applications will effectively target in particular supersonic flows in aerodynamics [3, 64] and astrophysics [30, 55, 52], as well as fluid-structure interaction problems [4, 40, 24].

References

1. Rémi Abgrall, Philipp Öffner, and Hendrik Ranocha. Reinterpretation and extension of entropy correction terms for residual distribution and discontinuous galerkin schemes: Application to structure preserving discretization. *Journal of Computational Physics*, 453:110955, 2022.
2. Robert W Anderson, Veselin A Dobrev, Tzanio V Kolev, Robert N Rieben, and Vladimir Z Tomov. High-order multi-material ale hydrodynamics. *SIAM Journal on Scientific Computing*, 40(1):B32–B58, 2018.
3. Antonios Antoniadis, Panagiotis Tsoutsanis, and Dimitrios Drikakis. High-order schemes on mixed-element unstructured grids for aerodynamic flows. In *42nd AIAA Fluid Dynamics Conference and Exhibit*, page 2833, 2012.
4. Steffen Basting, Annalisa Quaini, Suncica Canic, and Roland Glowinski. Extended ale method for fluid–structure interaction problems with large structural displacements. *Journal of Computational Physics*, 331:312–336, 2017.
5. W. Bo and M.J. Shashkov. Adaptive reconnection-based arbitrary Lagrangian Eulerian method. *Journal of Computational Physics*, 299:902–939, 2015.
6. W. Boscheri, M. Dumbser, and O. Zanotti. High order cell-centered Lagrangian-type finite volume schemes with time-accurate local time stepping on unstructured triangular meshes. *Journal of Computational Physics*, 291:120–150, 2015.
7. Walter Boscheri, Simone Chiocchetti, and Ilya Peshkov. A cell-centered implicit-explicit lagrangian scheme for a unified model of nonlinear continuum mechanics on unstructured meshes. *Journal of Computational Physics*, 451:110852, 2022.
8. Walter Boscheri and Michael Dumbser. Arbitrary-lagrangian-eulerian one-step weno finite volume schemes on unstructured triangular meshes. *Communications in Computational Physics*, 14(5):1174–1206, 2013.
9. Walter Boscheri, Michael Dumbser, and Elena Gaburro. Continuous finite element subgrid basis functions for discontinuous galerkin schemes on unstructured polygonal voronoi meshes. *Communications in Computational Physics*, 32(1):259–298, 2022.

10. E.J. Caramana and M.J. Shashkov. Elimination of artificial grid distorsion and hourglass–type motions by means of Lagrangian subzonal masses and pressures. *Journal of Computational Physics*, 142:521–561, 1998.
11. G. Carré, S. Del Pino, B. Després, and E. Labourasse. A cell-centered Lagrangian hydrodynamics scheme on general unstructured meshes in arbitrary dimension. *Journal of Computational Physics*, 228:5160–5183, 2009.
12. Manuel Castro, José M Gallardo, Juan A López-GarcÍa, and Carlos Parés. Well-balanced high order extensions of godunov's method for semilinear balance laws. *SIAM Journal on Numerical Analysis*, 46(2):1012–1039, 2008.
13. Simone Chiocchetti and Christoph Müller. A solver for stiff finite-rate relaxation in baer–nunziato two-phase flow models. In *Droplet Interactions and Spray Processes*, pages 31–44. Springer, 2020.
14. Simone Chiocchetti, Ilya Peshkov, Sergey Gavrilyuk, and Michael Dumbser. High order ader schemes and glm curl cleaning for a first order hyperbolic formulation of compressible flow with surface tension. *Journal of Computational Physics*, 426:109898, 2021.
15. S. Clain, S. Diot, and R. Loubère. A high-order finite volume method for systems of conservation laws—multi-dimensional optimal order detection (MOOD). *Journal of Computational Physics*, 230(10):4028–4050, 2011.
16. Bruno Després. *Numerical methods for Eulerian and Lagrangian conservation laws*. Birkhäuser, 2017.
17. V.A. Dobrev, T.E. Ellis, Tz.V. Kolev, and R.N. Rieben. High order curvilinear finite elements for axisymmetric Lagrangian hydrodynamics. *Computers and Fluids*, 83:58–69, 2013.
18. Veselin Dobrev, Patrick Knupp, Tzanio Kolev, Ketan Mittal, Robert Rieben, and Vladimir Tomov. Simulation-driven optimization of high-order meshes in ale hydrodynamics. *Computers & Fluids*, 208:104602, 2020.
19. M. Dumbser. Arbitrary–Lagrangian–Eulerian ADER–WENO finite volume schemes with time–accurate local time stepping for hyperbolic conservation laws. *Computer Methods in Applied Mechanics and Engineering*, 280:57–83, 2014.
20. M. Dumbser and D. S. Balsara. A new efficient formulation of the HLLEM Riemann solver for general conservative and non-conservative hyperbolic systems. *Journal of Computational Physics*, 304(C):275–319, 2016.
21. Michael Dumbser, Dinshaw S Balsara, Eleuterio F Toro, and Claus-Dieter Munz. A unified framework for the construction of one-step finite volume and discontinuous galerkin schemes on unstructured meshes. *Journal of Computational Physics*, 227(18):8209–8253, 2008.
22. Michael Dumbser, Simone Chiocchetti, and Ilya Peshkov. On numerical methods for hyperbolic pde with curl involutions. In *Continuum Mechanics, Applied Mathematics and Scientific Computing: Godunov's Legacy*, pages 125–134. Springer, 2020.
23. Michael Dumbser, Francesco Fambri, Elena Gaburro, and Anne Reinarz. On glm curl cleaning for a first order reduction of the ccz4 formulation of the einstein field equations. *Journal of Computational Physics*, page 109088, 2019.
24. Jakob Dürrwächter, Marius Kurz, Patrick Kopper, Daniel Kempf, Claus-Dieter Munz, and Andrea Beck. An efficient sliding mesh interface method for high-order discontinuous galerkin schemes. *Computers & Fluids*, 217:104825, 2021.
25. Francesco Fambri, Michael Dumbser, and Olindo Zanotti. Space–time adaptive ader-dg schemes for dissipative flows: Compressible navier–stokes and resistive mhd equations. *Computer Physics Communications*, 220:297–318, 2017.
26. A-A Gabriel, Duo Li, Simone Chiocchetti, Maurizio Tavelli, Ilya Peshkov, Evgeniy Romenski, and Michael Dumbser. A unified first-order hyperbolic model for nonlinear dynamic rupture processes in diffuse fracture zones. *Philosophical Transactions of the Royal Society A*, 379(2196):20200130, 2021.
27. Elena Gaburro. A unified framework for the solution of hyperbolic pde systems using high order direct arbitrary-lagrangian–eulerian schemes on moving unstructured meshes with topology change. *Archives of Computational Methods in Engineering*, 28(3):1249–1321, 2021.

28. Elena Gaburro, Walter Boscheri, Simone Chiocchetti, Christian Klingenberg, Volker Springel, and Michael Dumbser. High order direct arbitrary-lagrangian-eulerian schemes on moving voronoi meshes with topology changes. *Journal of Computational Physics*, 407:109167, 2020.
29. Elena Gaburro, Manuel J Castro, and Michael Dumbser. A well balanced diffuse interface method for complex nonhydrostatic free surface flows. *Computers & Fluids*, 175:180–198, 2018.
30. Elena Gaburro, Manuel J Castro, and Michael Dumbser. A well balanced finite volume scheme for general relativity. *SIAM Journal on Scientific Computing*, 43(6):B1226–B1251, 2021.
31. Elena Gaburro and Michael Dumbser. A posteriori subcell finite volume limiter for general pnpm schemes: Applications from gasdynamics to relativistic magnetohydrodynamics. *Journal of Scientific Computing*, 86(3):1–41, 2021.
32. Elena Gaburro, Michael Dumbser, and Manuel J Castro. Direct arbitrary-lagrangian-eulerian finite volume schemes on moving nonconforming unstructured meshes. *Computers & Fluids*, 159:254–275, 2017.
33. Elena Gaburro, Philipp Öffner, Mario Ricchiuto, and Davide Torlo. High order entropy preserving ader scheme. *arXiv preprint arXiv:2206.03889*, 2022.
34. S.K. Godunov. Finite difference methods for the computation of discontinuous solutions of the equations of fluid dynamics. *Mathematics of the USSR: Sbornik*, 47:271–306, 1959.
35. Jean-Luc Guermond, Murtazo Nazarov, Bojan Popov, and Ignacio Tomas. Second-order invariant domain preserving approximation of the euler equations using convex limiting. *SIAM Journal on Scientific Computing*, 40(5):A3211–A3239, 2018.
36. C. Hu and C.W. Shu. A high-order weno finite difference scheme for the equations of ideal magnetohydrodynamics. *Journal of Computational Physics*, 150:561 – 594, 1999.
37. R. Käppeli and S. Mishra. Well-balanced schemes for the euler equations with gravitation. *Journal of Computational Physics*, 259:199–219, 2014.
38. Friedemann Kemm, Elena Gaburro, Ferdinand Thein, and Michael Dumbser. A simple diffuse interface approach for compressible flows around moving solids of arbitrary shape based on a reduced baer–nunziato model. *Computers & fluids*, 204:104536, 2020.
39. Mack Kenamond, Dmitri Kuzmin, and Mikhail Shashkov. A positivity-preserving and conservative intersection-distribution-based remapping algorithm for staggered ale hydrodynamics on arbitrary meshes. *Journal of Computational Physics*, 435:110254, 2021.
40. Evgeny Kikinzon, Mikhail Shashkov, and Rao Garimella. Establishing mesh topology in multi-material cells: Enabling technology for robust and accurate multi-material simulations. *Computers & Fluids*, 172:251–263, 2018.
41. Christian Klingenberg, Gabriella Puppo, and Matteo Semplice. Arbitrary order finite volume well-balanced schemes for the euler equations with gravity. *SIAM Journal on Scientific Computing*, 41(2):A695–A721, 2019.
42. W. Liu, J. Cheng, and C.W. Shu. High order conservative Lagrangian schemes with Lax–Wendroff type time discretization for the compressible Euler equations. *Journal of Computational Physics*, 228:8872–8891, 2009.
43. R. Loubère, P. H. Maire, and P. Váchal. 3D staggered Lagrangian hydrodynamics scheme with cell-centered Riemann solver-based artificial viscosity. *International Journal for Numerical Methods in Fluids*, 72:22 – 42, 2013.
44. R. Loubère, P. H. Maire, and M.J. Shashkov. ReALE: A Reconnection Arbitrary-Lagrangian–Eulerian method in cylindrical geometry. *Computers and Fluids*, 46:59–69, 2011.
45. R. Loubère, P. H. Maire, M.J. Shashkov, J. Breil, and S. Galera. ReALE: A reconnection-based arbitrary-Lagrangian–Eulerian method. *Journal of Computational Physics*, 229:4724–4761, 2010.
46. R. Loubère and M.J. Shashkov. A subcell remapping method on staggered polygonal grids for arbitrary–lagrangian–eulerian methods. *Journal of Computational Physics*, 23:155–160, 2004.
47. Raphaël Loubere, Michael Dumbser, and Steven Diot. A new family of high order unstructured mood and ader finite volume schemes for multidimensional systems of hyperbolic conservation laws. *Communications in Computational Physics*, 16(3):718–763, 2014.

48. P.H. Maire. A unified sub-cell force-based discretization for cell-centered Lagrangian hydrodynamics on polygonal grids. *International Journal for Numerical Methods in Fluids*, 65:1281–1294, 2011.

49. Nathaniel R Morgan and Billy J Archer. On the origins of lagrangian hydrodynamic methods. *Nuclear Technology*, 207(sup1):S147–S175, 2021.

50. Nathaniel R Morgan, Xiaodong Liu, and Donald E Burton. Reducing spurious mesh motion in lagrangian finite volume and discontinuous galerkin hydrodynamic methods. *Journal of Computational Physics*, 372:35–61, 2018.

51. C.D. Munz. On Godunov–type schemes for Lagrangian gas dynamics. *SIAM Journal on Numerical Analysis*, 31:17–42, 1994.

52. H Olivares, IM Peshkov, ER Most, FM Guercilena, and LJ Papenfort. New first-order formulation of the einstein equations exploiting analogies with electrodynamics. *Physical Review D*, 105(12):124038, 2022.

53. Carlos Parés. Numerical methods for nonconservative hyperbolic systems: a theoretical framework. *SIAM Journal on Numerical Analysis*, 44(1):300–321, 2006.

54. Ilya Peshkov, Michael Dumbser, Walter Boscheri, Evgeniy Romenski, Simone Chiocchetti, and Matteo Ioriatti. Simulation of non-newtonian viscoplastic flows with a unified first order hyperbolic model and a structure-preserving semi-implicit scheme. *Computers & Fluids*, 224:104963, 2021.

55. Ilya Peshkov, Evgeniy Romenski, and Michael Dumbser. Continuum mechanics with torsion. *Continuum Mechanics and Thermodynamics*, 31(5):1517–1541, sep 2019.

56. Barbara Re, Cecile Dobrzynski, and Alberto Guardone. An interpolation-free ale scheme for unsteady inviscid flows computations with large boundary displacements over three-dimensional adaptive grids. *Journal of Computational Physics*, 340:26–54, 2017.

57. J. Ruppert. A new and simple algorithm for quality 2-dimensional mesh generation. *Proceedings of the 4th ACM-SIAM Symposium on Discrete Algorithms*, pages 83–92, 1993.

58. V. V. Rusanov. Calculation of Interaction of Non–Steady Shock Waves with Obstacles. *J. Comput. Math. Phys. USSR*, 1:267–279, 1961.

59. G. Scovazzi. Lagrangian shock hydrodynamics on tetrahedral meshes: A stable and accurate variational multiscale approach. *Journal of Computational Physics*, 231:8029–8069, 2012.

60. L.I. Sedov. *Similarity and Dimensional Methods in Mechanics*. Academic Press, New York, 1959.

61. Volker Springel. E pur si muove: Galilean-invariant cosmological hydrodynamical simulations on a moving mesh. *Monthly Notices of the Royal Astronomical Society*, 401(2):791–851, 2010.

62. Maurizio Tavelli, Simone Chiocchetti, Evgeniy Romenski, Alice-Agnes Gabriel, and Michael Dumbser. Space-time adaptive ader discontinuous galerkin schemes for nonlinear hyperelasticity with material failure. *Journal of computational physics*, 422:109758, 2020.

63. Eleuterio F Toro. *Riemann solvers and numerical methods for fluid dynamics: a practical introduction*. Springer Science & Business Media, 2013.

64. Panagiotis Tsoutsanis, Ioannis W Kokkinakis, László Könözsy, Dimitris Drikakis, Robin JR Williams, and David L Youngs. Comparison of structured-and unstructured-grid, compressible and incompressible methods using the vortex pairing problem. *Computer Methods in Applied Mechanics and Engineering*, 293:207–231, 2015.

65. J. von Neumann and R.D. Richtmyer. A method for the calculation of hydrodynamics shocks. *Journal of Applied Physics*, 21:232–237, 1950.

66. Luming Wang and Per-Olof Persson. A high-order discontinuous galerkin method with unstructured space–time meshes for two-dimensional compressible flows on domains with large deformations. *Computers & Fluids*, 118:53–68, 2015.

67. M. L. Wilkins. Calculation of elastic-plastic flow. *Methods in Computational Physics*, 3, 1964.